UC Berkeley
UC Berkeley Previously Published Works

Title

Size Transformation of the Au22(SG)18 Nanocluster and Its Surface-Sensitive Kinetics

Permalink

https://escholarship.org/uc/item/3z8237vc

Journal

Journal of the American Chemical Society, 142(26)

ISSN

0002-7863

Authors

Zhang, Bei
Chen, Chubai
Chuang, Wesley
et al.

Publication Date

2020-07-01

DOI

10.1021/jacs.0c03919

Peer reviewed

Size transformation of $Au_{22}(SG)_{18}$ nanocluster and its surface sensitive ~~dynamics~~kinetics

Bei Zhang, Chubai Chen, Wesley Chuang, Shouping Chen, Peidong Yang*

Department of Chemistry, University of California, Berkeley, California 94720, United States

ABSTRACT: For many applications of well-defined gold nanoclusters, it's desirable to understand their structural evolution behavior under working conditions with molecular precision. Here we report the first systematic investigation on the size transformation product of $Au_{22}(SG)_{18}$ nanocluster under representative working conditions and highlight the surface effect on the transformation dynamics. Under thermal and aerobic conditions, the consecutive and pH dependent transformation from Au_{22} to both well-defined clusters and small Au(I)SR species were identified by the ESI-MS and UV-vis spectroscopy. By introducing perturbation on the Au_{22} surface, significant changes in the activation parameters were determined from the kinetic study of the Au_{22} transformation. This indicates the sensitivity of nanocluster transformation pathway the cluster surface. The systematic study on cluster transformation and sensitivity of cluster transformation to the surface revealed herein have significant implications for future attempts to design gold nanoparticles with adaptation to the working environment and the regeneration of active nanoparticles.

INTRODUCTION

Thiolate protected gold nanoclusters with 10 to a few hundred gold atoms have shown great potential for catalysis, energy and biomedical applications.[1] Gold nanoclusters possess atomically precise core-shell structure. Change in the number of gold atoms significantly affects their structure, properties and therefore practical applications. In gold nanocluster sensitized solar cells, Au_{18} demonstrated the highest solar to power efficiency among Au_{10}, Au_{15}, Au_{18} and Au_{25} nanoclusters, benefiting from its interfacial events such as charge injection kinetics, interfacial charge recombination, and charge transport.[2] With the increase of few gold atoms, the renal clearance of gold nanoclusters was slowed down four to nine fold in Au_{25} than in Au_{18}, Au_{15} and Au_{10-12} nanoclusters.[3] Furthermore, the catalytic activity of gold nanoclusters increases with the cluster size in various oxidation and reduction reactions. The conversion/turn over frequency follows the order: Au_{144}> Au_{38}> Au_{25}, which is related with the increased surface area of gold nanoclusters.[4-6] Among them, Jin and coworkers reported the size change of nanocluster (Au_{15}, Au_{18}, Au_{25} and Au_{38}) after hydrogenation of 4-nitrobenzaldehyde by polyacrylamide gel electrophoresis (PAGE) analysis of post reaction catalysts.[6] The Au(I)-SR species generated in situ from oxidative decomposition of Au_{25} were identified as catalytically active sites in styrene oxidation reaction.[7] Due to the sensitivity of the cluster properties to the size of nanoclusters, it is essential to study the stability of gold nanoclusters at atomic level under working conditions (thermal, wide pH range, presence of reactive molecules, etc.).

In spite of the superior air and moisture stability of gold nanocluster than other metal nanoclusters (Ag, Cu, etc.)[1], the stability of gold nanocluster in harsh conditions remains mysterious. Racemization of the $Au_{38}(SR)_{24}$[8] and $Au_{40}(SR)_{24}$[9] enantiomers have been observed upon heating, indicating the flexibility of gold nanocluster. Furthermore, thermal etching with[10,11] or without[12] excessive foreign thiol ligands, oxidative[13], reductive[14-16] and acidic[17] conditions are able to activate the transformation of nanocluster from one stable size to another stable size. The amount/structure of foreign ligand, temperature, and pH value are critical parameters for inducing the size transformation of gold nanoclusters. However, the generality of the size transformation products has not been investigated systematically. Both surface rearrangement[8,10] and core reconstruction[18] mechanisms have been hypothesized for the size transformation and racemization processes. The detailed transformation pathway remains elusive since most reported size transformation studies on $Au_n(SR)_m$ nanoclusters focus on the starting and final nanocluster species.

The $Au_{22}(SG)_{18}$ (GSH: glutathione) nanocluster has been used for solar CO_2 reduction, bioimaging, and mimicking the pathogenic invasion owing to its photoluminescence, biocompatibility and ability to harvest visible

light.[19-22] The gold nanocluster in energy and biological applications is exposed to thermal condition, cellular thiol and broad pH range, which could potentially affect the cluster size. In this work, we have studied the generality of $Au_{22}(SG)_{18}$ size transformation and the role of cluster surface on the transformation pathway. We have systematically mapped out the size transformation of $Au_{22}(SG)_{18}$ in wide pH range and in presence of free GSH at different temperatures. The ESI-MS analysis and UV-vis spectra show that thermal transformation under air maintained/lowered the free valence electron and lowered the Au/SR ratio, related to increased surface gold percentage or longer surface units. Size transformation of $Au_{22}(SG)_{18}$ is independent on the temperature in the performed studies. The activation parameters of Au_{22} transformation under the performed conditions were calculated by following the transformation kinetics. The drastic decrease in transformation energy barrier and change in product size upon changing the ligand sodium number and adding free thiol reveal the sensitivity of cluster transformation to the cluster surface.

EXPERIMENTAL SECTION

Materials. Tetrachloroauric (III) acid ($HAuCl_4 \cdot 3H_2O$, >99.99% metals basis), L-glutathione reduced and sodium borohydride ($NaBH_4$, 99%) were received from Sigma Aldrich. Sodium hydroxide (NaOH), hydrochloric acid (HCl) and methanol were obtained from Fisher Chemical. Water was deionized with the Millipore Milli-Q UF Plus system.

Synthesis of $Au_{22}(SG)_{18}$ nanocluster. $Au_{22}(SG)_{18}$ nanocluster has been prepared by modified protocol from Xie's report. $HAuCl_4 \cdot 3H_2O$ (12.5 mM) and glutathione (7.5 mM) were dissolved in 180 mL H_2O under vigorous stirring. The solution changed from light yellow to white turbid in 2min. The pH of the reaction solution was then adjusted to 12 by NaOH (1M) aqueous solution and left a transparent solution. Afterwards, the freshly prepared $NaBH_4$ (100mM, 6mL) solution was added at once under 500 rpm stirring. The solution color changed gradually to orange red within 30 min. HCl (0.33M) was used to adjust the solution to pH 2.5 and the stirring was kept at 500 rpm for 8h. The solid crude product was obtained by adding 0.5 equivalent volume of methanol and subsequent centrifuge precipitation at 8000 rpm for 10 min. The isolation of Au_{22} nanocluster has been carried out by fractional precipitation from saturate crude aqueous solution using methanol. The purity of the isolated sample has been confirmed from UV-vis and ESI-MS.

$Au_{22}(SG)_{18}$ transformation. $Au_{22}(SG)_{18}$ solution (0.15 mg/mL, determined by ICP-AES; pH 5.25, confirmed by pH meter) was prepared and divided into 4 batches, which were heated at 35°C, 43.5 °C, 52 °C, and 60 °C, respectively. UV-vis spectra of the 4 solutions was recorded at different time intervals due to the varied reaction rate: every 12 h at 35°C, every hour from 0 h to 16 h and every 7 h from 16 h to 107 h at 43.5 °C, every hour from 0 h to 18 h at 52 °C, and every hour from 0 h to 9 h at 60 °C. The following samples were collected over the course of $Au_{22}(SG)_{18}$ nanocluster transformation. 1. $Au_{22}(SG)_{18}$ nanocluster from synthesis. 2. Sample after heating the $Au_{22}(SG)_{18}$ (pH 5.25) at 60 °C for 9 h. 3. Sample after heating the $Au_{22}(SG)_{18}$ (pH 5.25) at 60 °C for 107 h. Centrifugation filtration with the cut-off at 3000 g/mol was subsequently applied, rendering two batches of cluster with the expected molecular weight >3000 g/mol and <3000 g/mol. Both UV-vis and ESI-MS have been employed for the above samples. PAGE has been applied to study the size of sample 3.

pH effect study. $Au_{22}(SG)_{18}$ (pH 8) was prepared by dissolving the $Au_{22}(SG)_{18}$ solid sample by NaOH aqueous solution (10^{-6} M). $Au_{22}(SG)_{18}$ (pH 8) solution (0.18 mg/mL, determined by ICP-AES) was prepared and divided into 3 batches, which were heated at 45 °C, 52 °C, and 59.5 °C, respectively. UV-vis spectra of the 3 solutions was recorded every 30 min for 4.5 hours. The starting Au_{22} (pH 8) sample and the solution collected at 4.5h, 59.5 °C were characterized by ESI-MS. $Au_{22}(SG)_{18}$ (pH 2.52) was prepared by dissolving the solid $Au_{22}(SG)_{18}$ solid sample with HCl (pH ~2) and the final pH of the solution was determined by pH meter.

Free thiol experiment. To a solution of $Au_{22}(SG)_{18}$ (0.1 mg, 0.9 mL), glutathione solution (0.312 mg, 0.1 mL; $n_{glutathione}:n_{Au22}$ = 100:1) was added and heated at 73 °C. The UV-vis of the mixture was recorded at 25 min and 50 min. The same solutions were prepared and heated at 34.5 °C, 43.5 °C, 52 °C, and 60 °C and characterized by UV-vis ~every 25 min for kinetic study and calculation of activation parameters. To a solution of $Au_{22}(SG)_{18}$ (0.1 mg, 0.9 mL), glutathione solution (0.062 mg, 0.1 mL; $n_{glutathione}:n_{Au22}$ = 20:1) was added and heated at 52 °C, 60 °C and 73 °C. The UV-vis of the mixture was recorded ~every 25 min.

Characterizations. UV-vis spectrometer spectra were recorded on UV-vis spectrophotometer (UV-3101, Shimazu) at room temperature. Electrospray ionization (ESI) mass spectra were recorded using a Waters Q-TOF mass spectrometer equipped with Z-spray source. The source temperature was kept at 70 °C. The sample was directly infused into the chamber at 5 μL/ min. The spray voltage was kept at 2.20 kV and the cone voltage at 60 V. The ESI sample was dissolved in water (~1 mg/mL) before injection. All the spectra were obtained with negative ion mode in the m/z range from 400 to 2000. Polyacrylamide gel electrophoresis (PAGE) was carried out on a BIO-RAD MiniProtean unit, using 30 wt% separation gel (acrylamide/Bis, 19:1) with

a 1.5 mm spacer. The eluting buffer contained 192 mM glycine and 25 mM tris. Samples were dissolved in 5% (v/v) glycerol-water, loaded and eluted at 150 V for 3h at room temperature. Inductively coupled plasma atomic emission spectroscopy (ICP-AES) was carried out on a PerkinElmer optical emission spectrometer (Optima 7000 DV). Before the ICP-AES measurement, the solid gold cluster/complex was digested in aqua regia for 24 h, and then deionized water was added to dilute the solution to a suitable concentration

Determination of isolated nanocluster concentration. The concentration dependent UV-vis absorbance of individual gold nanoclusters has been calibrated. The plot of nanocluster concentration over absorption intensity (Au_{22}@515.5 nm and Au_{18}@623 nm) gives a good linear fit. Note: The wavelength of 515.5 nm is chosen for Au_{22} absorption study as it is the characteristic absorption. The characteristic absorption wavelength of 623 nm is chosen for Au_{18} absorption study in order to avoid overlap with other nanoclusters (Au_{22}, final Au_n cluster, etc.).

Determination of nanocluster concentration during transformation. 1. Au_{22} concentration during Au_{22} to Au_{18} transformation. The concentration of Au_{22} nanocluster during the Au_{22} transformation has been calibrated from its UV-vis absorption intensity. Since the absorption peaks of Au_{22} and Au_{18} overlap at 515.5 nm. The absorption of Au_{22} at 515.5 nm has been determined by subtracting the absorption of Au_{18} nanocluster from the total absorption at the same wavelength. The absorption of Au_{18} at 515.5 nm was calculated from its absorption at 623 nm. 2. Au_{18} concentration during Au_{18} transformation. The concentration of Au_{18} was calculated from the UV absorption at 623 nm since its absorption doesn't overlap with the final product. 3. Au_{22} concentration during Au_{22} to Au_{15} transformation. The concentration of Au_{22} was calculated from the UV absorption at 515 nm since its absorption at this wavelength doesn't overlap with Au_{15}. 4. Activation parameters. The reaction constant of nanocluster transformation reaction was obtained by plotting ln(c) over time. Activation parameters (Ea, $\Delta H^{\square}$, $\Delta S^{\square}$, and $\Delta G^{\square}$) has been calculated according to Eyring plot and Arrhenius plot.

RESULTS AND DISCUSSION

Transformation of $Au_{22}(SG)_{18}$ nanocluster. $Au_{22}(SG)_{18}$ nanocluster has been prepared and isolated by modifying the reported synthesis.[19] The characteristic peaks in UV-vis (460 and 515 nm) and the ESI-MS spectra (m/z 1093 [$Au_{22}(SG)_{18}$ - $9H^+]^{9-}$; m/z 1229 [$Au_{22}(SG)_{18}$ - $8H^+]^{8-}$; m/z 1405 [$Au_{22}(SG)_{18}$ - $7H^+]^{7-}$; and m/z 1640 $Au_{22}(SG)_{18}$ - $6H^+]^{6-}$) agreed with literature (Figure 1, Figure S1).[19] Additional minor peaks in ESI-MS spectrum were also observed at m/z 1212.7 (z = 8), 1364.4 (z = 7) and 1565.4 (z = 6), which corresponds to

the molecular weight of 9765, 9599.8 and 9428 g/mol. Considering the molecular weight of $Au_{22}(SG)_{18}$ (9847 g/mol) and GSH (307 g/mol), these species were possibly generated from the decomposition of the protecting thiolate ligands on $Au_{22}(SG)_{18}$ nanocluster during ESI measurement. The aqueous solution of the isolated $Au_{22}(SG)_{18}$ nanocluster was prepared (pH 5.25). UV-vis was applied to monitor the solution upon heating at 60 °C (Figure 1a). The intensity of its characteristic absorption peaks at 460 nm and 515 nm decrease significantly upon heating. Meanwhile new set of peaks at 450 nm, 568 nm and 623 nm appear and reach the maximum intensity after heating for ~9 h. These new peaks in UV-vis spectra could be assigned to $Au_{18}(SG)_{14}$ nanocluster according to the report from Xie group[19] and Negishi group[23]. The presence of $Au_{18}(SG)_{14}$ nanocluster in the solution at 9 h is further confirmed by the ESI-MS peaks at m/z 1118 ([$Au_{18}(SG)_{14}$ - $7H^+]^{7-}$) and m/z 1304 ([$Au_{18}(SG)_{14}$ - $6H^+]^{6-}$) (Figure 1b). The experimental isotope distribution of [$Au_{18}(SG)_{14}$ - $7H^+]^{7-}$ is consistent with the simulated isotope distribution (Figure S1). Both ESI and ICP-AES were applied in order to understand fate of other four gold atoms in $Au_{22}(SG)_{18}$. No bigger nanocluster species were displayed in the range of 1100 – 2000 m/z in ESI-MS spectrum. Small Au(I)-thiolate species including [$Au(SG)_2]^-$, [$Au_2(SG)_3]^-$, $Au_3(SG)_3$, $Au_4(SG)_3$, $Au_4(SG)_4$ were observed in the range of 600 – 1000 m/z (Figure S2a). To further study if these small species were formed from ESI fragmentation, small species were isolated for complementary information. The solution at 9 h was further subjected to centrifuge filtration (cut-off: 3000 g/mol) to isolate the < 3000 g/mol species. ICP-AES confirmed the existence of gold atom in the small species, while exact quantification is not applicable due to the incomplete filtration. ESI-MS of the filtered small species shows the peaks under 800 m/z. The only identified gold-glutathione containing species in the sample is AuSG (Figure S2b, m/z 503.2, [$AuSG-H^+]^-$), which is complementary to the small species detected in the as obtained solution.

The UV-vis spectra of the $Au_{22}(SG)_{18}$ solution was recorded under three lower temperatures: 35°C, 43.5 °C and 52 °C at selected time intervals (Figure S3). The UV-vis spectra show the transformation of $Au_{22}(SG)_{18}$ nanocluster to $Au_{18}(SG)_{14}$ nanocluster at all the performed temperatures (Figure S3), suggesting the same transformation pathway. ~~This is in contrast to the temperature dependent size transformation from Au_{25} to Au_{28} (80 °C) and Au_{20} (40 °C).[24,25]~~
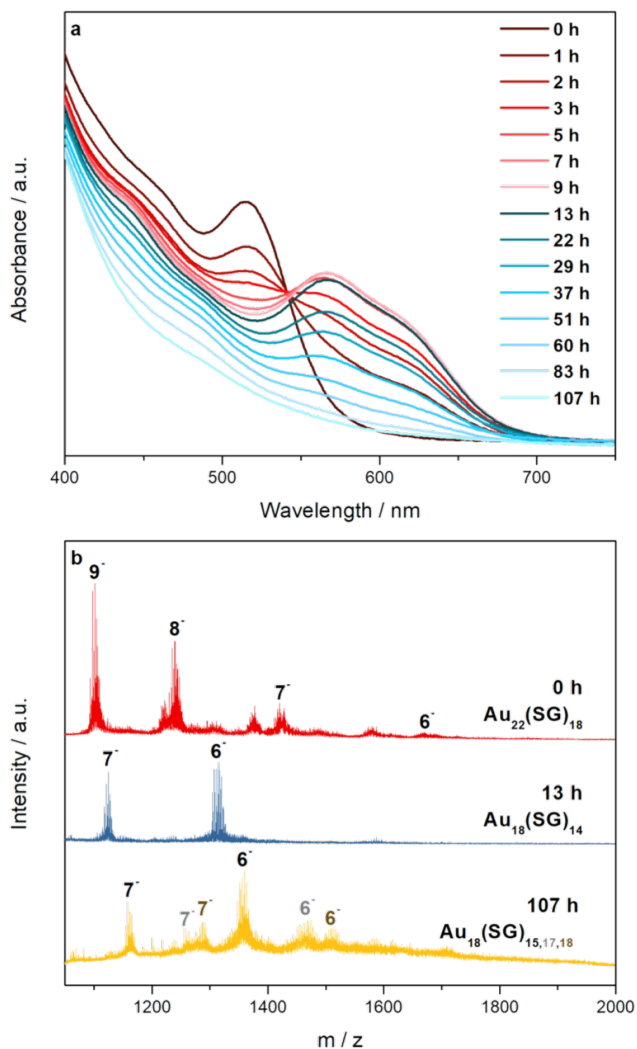
Figure 1. The in situ transformation of $Au_{22}(SG)_{18}$ upon heating at 60 $^\circ$C: (a) UV-vis and (b) ESI-MS. In the ESI spectra, the nanoclusters species have been identified and their charge has been marked above the corresponding peaks with the loss of corresponding number of H^+.

When the heating continued after 9 h at 60 °C, the absorption intensity of $Au_{18}(SG)_{14}$ at 520 nm and 623 nm gradually decrease and a new peak at ~ 484 nm has developed. The completion of $Au_{18}(SG)_{14}$ transformation was reached after an additional ~ 98 h. The UV-vis absorption at ~ 484 nm couldn't be assigned to any known size of glutathione
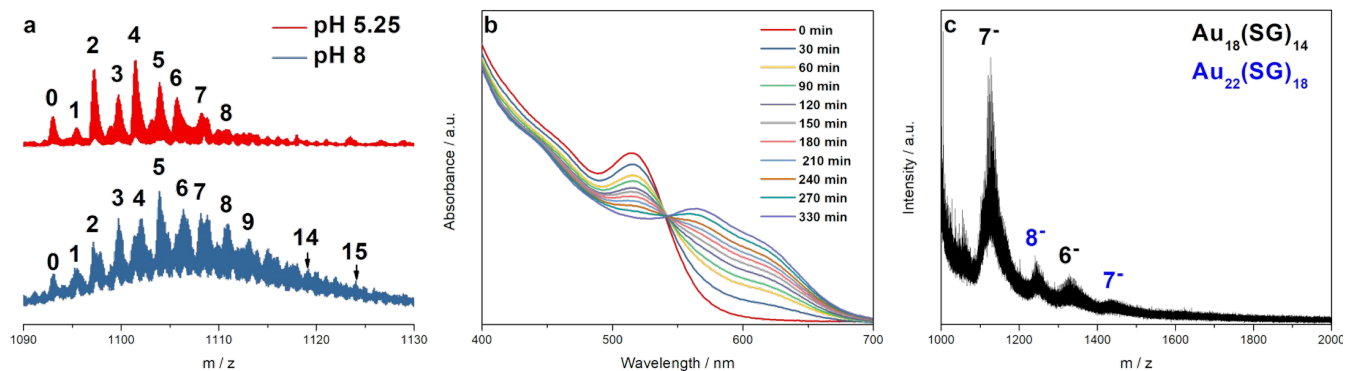
Figure 2. (a) ESI of $Au_{22}(SG)_{18}$ (pH5.25 and pH 8), charge z = 9. (b) In situ UV-vis of $Au_{22}(SG)_{18}$ transformation at pH 8. The solution temperature was kept at 59 °C. (c) ESI of $Au_{22}(SG)_{18}$ (pH8) solution at 330 min.

protected gold nanocluster. PAGE was firstly used to determine the component and relative size of the final product came between the band of $Au_{22}(SG)_{18}$ and $Au_{18}(SG)_{14}$, suggesting that the size of $Au_m(SG)_n$ lies between these two nanoclusters. ESI-MS spectrum of $Au_m(SG)_n$ displays three sets of peaks, which corresponding to $Au_{18}(SG)_{15}$, $Au_{18}(SG)_{17}$ and $Au_{18}(SG)_{18}$ (Figure 1b, Figure S4). Small Au-thiolate species including $Au(SG)_2$ and AuSG were observed in the range of 600 – 1000 m/z (Figure S5a). After centrifuge washing, ICP-AES confirmed the existence of gold atoms in < 3000 g/mol fraction. However, no Au-thiolate species could be assigned in the ESI-MS spectrum (Figure S5b). Continuous evolution of as isolated Au_{22} nanocluster aqueous solution upon heating was observed. In addition to the well-defined big nanocluster, small Au(I) species were also identified from both direct and centrifuge washed transformation solutions.

pH effect on the transformation of $Au_{22}(SG)_{18}$ nanocluster. By adjusting the pH of $Au_{22}(SG)_{18}$ nanocluster from pH 5.5 to pH 8, same set of $Au_{22}(SG)_{18}$ peaks were also observed in ESI (Figure S6), suggesting the cluster size is preserved. Figure 2a and Table S1 compare the sodium adduct species of the cluster in ESI spectra (z = 9). The increase of sodium atoms in pH 8 sample than in pH 5.25 sample is observed, where the maximum sodium number of which are 15 and 8 respectively. At 59 °C, transformation of $Au_{22}(SG)_{18}$ to $Au_{18}(SG)_{14}$ also occurred at pH 8, as observed by in situ UV-vis (Figure 2b, absorption peaks of Au_{18} at 450 nm, 568 nm and 623 nm) and ESI-MS spectrum (Figure 2c, ESI peaks of Au_{18} after losing 6 and 7 H^+ and isotopic distribution in Figure S7). Same transformation to $Au_{22}(SG)_{18}$ was suggested by in situ UV-vis at 45 °C, 52 °C and 59 °C (Figure S8). When acidic condition is applied to $Au_{22}(SG)_{18}$ nanocluster (pH 2.52), an immediate formation of $Au_{24}(SG)_{20}$ was identified by ESI (Figure S9). Change in the zwitterionic nature of glutathione ligands and intercluster hydrogen bond could be induced at different pH.[24] The pH dependent transformation pathway of $Au_{22}(SG)_{18}$ therefore favors the proposed surface induced size transformation mechanism, where the

transformation occurs from the exterior surface sites to the interior core.[10]

Free thiol mediated transformation of $Au_{22}(SG)_{18}$ nanocluster. The pH study suggests the surface effect on the nanocluster size transformation. An intriguing

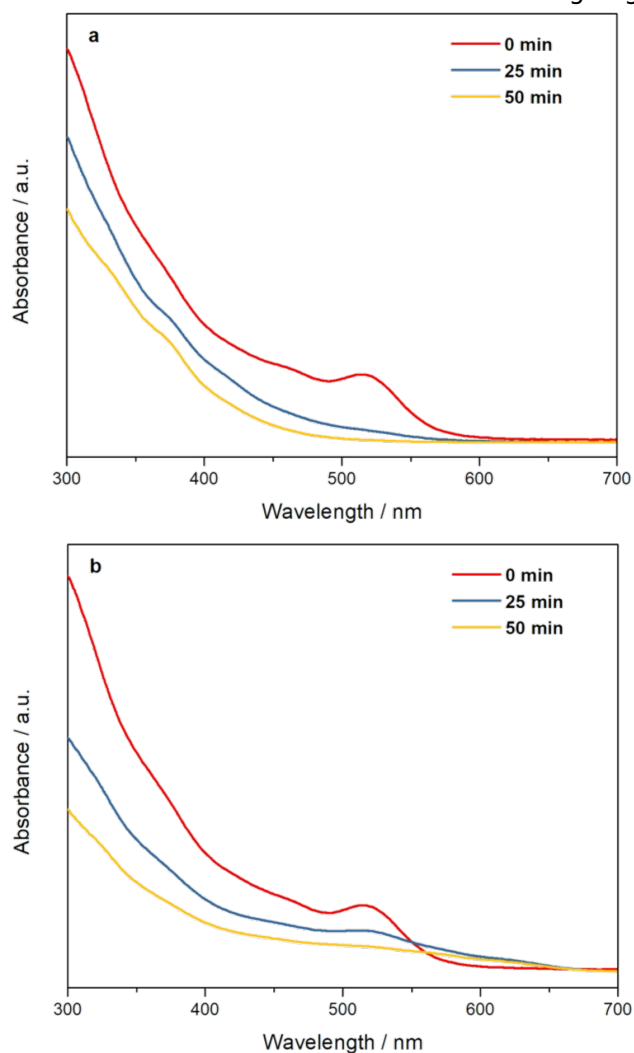**Figure 3.** In situ UV-vis of $Au_{22}(SG)_{18}$ transformation with (a) 5.5eq and (b) 1eq thiol. The solution temperature was kept at 73 °C.

question concerns if co-reactant can promote or alter the size transformation by interacting with the surface. The ligand induced size transformation has been excessively investigated by mixing nanocluster with a structurally different ligand, resulting in presumably a stable size unique to the new ligand. However, no study has been carried out using the same ligand. Furthermore, the glutathione is present in millimolar concentrations in the cell in biological applications. The transformation of $Au_{22}(SG)_{18}$ nanocluster was therefore studied in the presence of free glutathione thiol.

After adding ~ 5.5 eq GSH (comparing to the amount of thiolate ligand on Au22) to the aqueous solution of $Au_{22}(SG)_{18}$ and heat at 73 °C, the transformation product no longer shows the absorption feature of $Au_{18}(SG)_{14}$ (Figure 3a). Instead, new peaks at 376 nm and 419 nm evolve at 25 min, which correspond to the characteristic absorption of $Au_{15}(SG)_{13}$.[19] This assignment is furthered confirmed by the ESI spectra of the solution (Figure S10a, after losing 6 and 7 H^+). Subsequently, absorption peaks at 331 nm and 374 nm were observed in the solution after heating for 50 min, which could be assigned to $Au_{10-12}(SG)_{10-12}$ (Figure S10b). Similar trend of UV evolution was also observed after heating the aqueous solution of $Au_{22}(SG)_{18}$ at 34.5, 43.5, 52 and 60 °C (Figure S11).

When the amount of glutathione is lowered to ~1 equivalent to the ligand amount on $Au_{22}(SG)_{18}$, transformation to both $Au_{18}(SG)_{14}$ and $Au_{15}(SG)_{13}$ was observed at 73 °C by in situ UV (Figure 3b) and ESI (Figure S12), indicating the simultaneous transformation of pure Au_{22} and thiol mediated Au_{22} transformation.

The free thiol experiment suggests that the transformation products of $Au_{22}(SG)_{18}$ is altered by the presence of free thiol. Change in the transformation pathway is dependent on the thiol amount. Free glutathione ligand is expected to bind to gold atom from Au-S bond on the cluster surface and participate in the transformation pathway.

Interconversion between $Au_n(SG)_m$ nanoclusters. The transformation of pure and co-reactant mediated $Au_{22}(SG)_{18}$ transformation has been systematically mapped out (Scheme 1). Of note, transformation from Au_{22} to Au_{18} and Au_{15} has been identified herein. Reversibly, reduction growth from Au_{18} to Au_{22}[25] and Au_{15} to Au_{18}[26] with Au(I)-SR were also reported. Two parameters, transformation condition and structure of starting and final nanoclusters, could be employed to understand the generality of cluster size transformation.

In the case of cluster size growth under reductive conditions (eg. Au_{15} to Au_{18}[26] and Au_{18} to Au_{22}[25]), the number of free valence electrons in the cluster increase over time.[15,16] In contrast, free valence electrons in the transformation product of $Au_{22}(SG)_{18}$ (4e^-) either remains unchanged (Au_{18}/4e^-; Au_{24}/4e^-) or decreases (Au_{15}/2e^-; other secondary products Au_{10-12}/1e^-; Au_{18} with additional ligands/3, 1, 0e^-) under the performed conditions (heating in air). Conversion to Au_{15} could be ascribed to its high stability with magic electron number. The gold nanoclusters adopt Au core@ S-(Au-S)$_n$ (n= 0, 1, 2, …) structure. Since the crystal structure of most sizes in this study haven't been solved, the Au-to-SR ratio has been calculated for all the sizes for structure study. The Au-to-SR ratio decreases (except for the $Au_{18}(SG)_{14}$ product) after transformation, related with increased surface gold atom or long S-(Au-S)$_n$ surface staple. This could contribute to the energy balance between core and shell and therefore the cluster structural thermodynamic stabilization.[27]
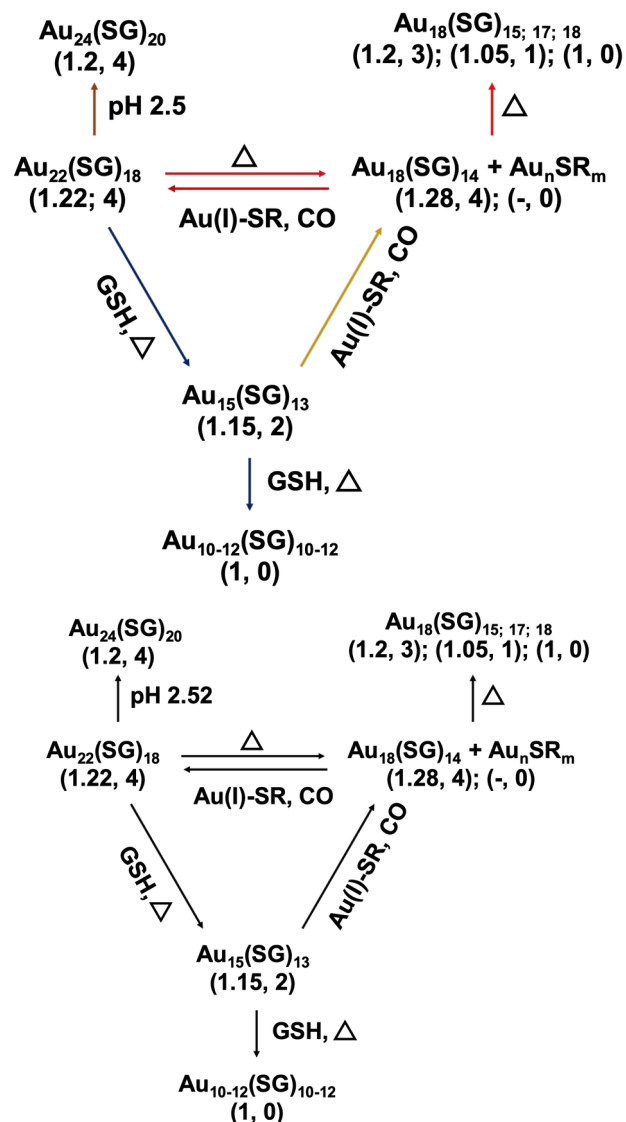
Scheme 1. Interconversion among glutathione protected gold nanoclusters. The (Au-to-SR ratio, number of free valence electrons) was marked below accordingly. The number of free valence electrons (n*) in [$Au_M(SR)_N$]^q is calculated with n*= M-N-q.

Activation parameters of Au$_{22}$(SG)$_{18}$ transformation. The kinetic studies were performed on the transformation of as isolated Au$_{22}$(SG)$_{18}$ nanocluster, Au$_{22}$(SG)$_{18}$ (pH 8) and Au$_{22}$(SG)$_{18}$ (with 5.5eq GSH) (details see experimental section). In general, a stock solution of nanocluster/(with GSH) was prepared and divided into equivalent batches. The concentration of the solution was determined by ICP-AES. UV-vis spectra of the solution were recorded over the heating process (Au$_{22}$, Figure 1, Figure S3; Au$_{22}$/pH8, Figure 2b, Figure S8; Au$_{22}$/GSH, Figure 3a, Figure S11). The absorption intensity of Au$_{22}$(SG)$_{18}$ nanocluster during transformation was calculated by subtracting the Au$_{18}$(SG)$_{14}$ absorption from the total absorption of transformation solution at 515.5 nm (Au$_{18}$ and smaller gold species show no absorption at this wavelength[15]). The concentration c of Au$_{22}$(SG)$_{18}$ nanocluster was calculated from the nanocluster concentration- UV absorption intensity calibration curve (Figure S13). Plot of ln (c) versus time in the three transformation processes yielded straight lines (Figure S14), indicating first-order kinetics. Rate constants k(T) were gained by determining the initial reaction rates by linear fits. The Eyring plot and Arrhenius plot (Figure 4) give linear fit and the activation energy is determined. Derived thermodynamic activation parameters ΔH$^{⧧}$, ΔS$^{⧧}$, and ΔG$^{⧧}$ are summarized in Table 1. obtained using same methods as in the case of Au$_{22}$(SG)$_{18}$ nanocluster (Table 1).

The activation energy Ea of as isolated Au$_{22}$(SG)$_{18}$ nanocluster transformation was determined to be 30.0 ± 2.2 kcal/mol. This is significantly lower than the gold-sulfur bond energy (50 kcal/mol)[28] and the calculated cohesive energy in ultrasmall Au$_n$ clusters (53-62 kcal/mol for n= 10-20)[29], suggesting simultaneous bond breaking and formation. The activation energy of Au$_{22}$ transformation is comparable to the activation energy required in the racemization of Au$_{38}$(SR)$_{24}$ nanoclusters (SR: phenylethanethiol, 22 kcal/mol;[8] SR: R-1,1'-binaphthyl-2,2'-dithiol partially substituted phenylethanethiol, 28 kcal/mol[30]) and Au$_{40}$(SR)$_{24}$ nanocluster (24.7 kcal/mol)[9], where both the surface rearrangement mechanism and core reconstruction mechanism[18] were proposed.

After adjusting the solution pH to 8, the activation energy showed significant decrease to 19.3 ± 1.5 kcal/mol. Meanwhile changes to negative entropy were observed (-21.4 ± 4.7 cal/mol/K), compared to the as isolated Au$_{22}$ cluster (12.1 ± 6.9 cal/mol/K). Alteration of the transformation pathway was therefore indicated, even though same transformation product Au$_{18}$ was identified. The sensitivity of the transformation pathway to the number of sodium number in the Au$_{22}$/Na adduct is also revealed. Adding free thiol to the as isolated Au$_{22}$ solution not only changes the transformation pathway and subsequent products (Au$_{15}$), but also significantly lowered the activation energy to 12.7 ± 0.7 kcal/mol. The drastic change in activation energy (>2-fold decrease) could be related with more Au-S bond formation in the transformation intermediates.
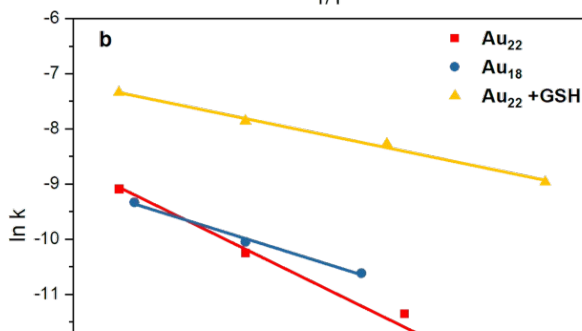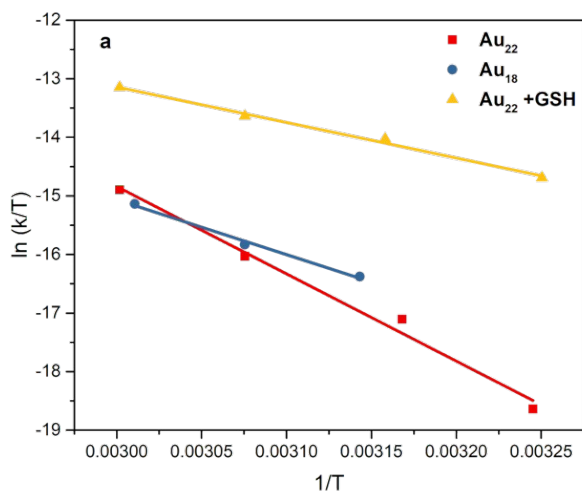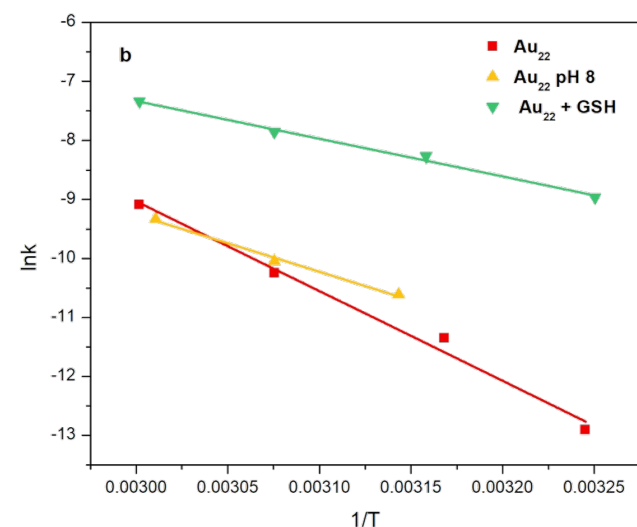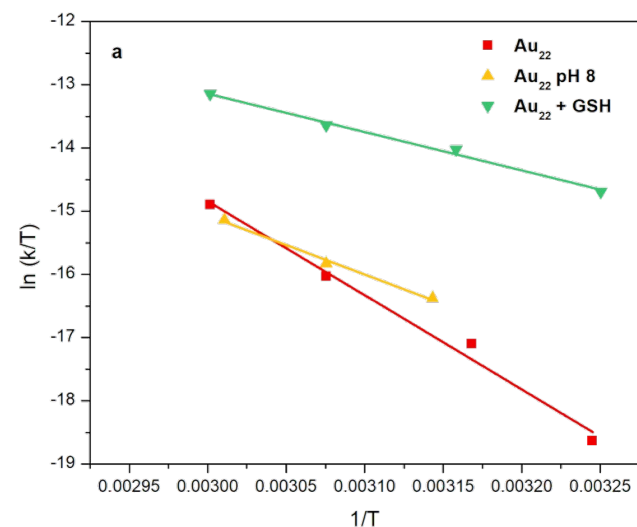
Figure 4. Determination of activation parameters of $Au_{22}(SG)_{18}$ transformation: (a) Eyring plot and (b) Arrhenius plot.

Table 1. Activation parameters of $Au_{22}(SG)_{18}$ transformation (T = 298.15 K).

Nanocluster	Ea kcal/mol	ΔH‡ kcal/mol	ΔS‡ cal/mol/K	ΔG‡ kcal/mol
Au_{22}	30.0 ± 2.2	29.6 ± 2.2	12.1 ± 6.9	25.0 ± 4.8
Au_{22} (pH 8)	19.3 ± 1.5	18.6 ± 1.5	-21.4 ± 4.7	26.6 ± 3.3
Au_{22} (GSH)	12.7 ± 0.7	12.1 ± 0.7	-37.2 ± 2.1	26.0 ± 1.5

Conclusions. In conclusion, size transformation of $Au_{22}(SG)_{18}$ nanocluster has been systematically investigated in wide pH range and presence of the same thiol ligand, resulting in both well-defined clusters (Au_{18}/pH5.25 and pH 8, Au_{24}/pH 2.5, Au_{15}/GSH) and small Au(I)SR species. The transformation products remain independent on the performed temperatures. The free valence electron maintained/decreased and the Au-to-SR ratio decreased under most of the performed conditions, which is in contrast to the size evolution of gold nanocluster under reductive conditions. The mapped interconversion of nanoclusters reveals the generality of the size transformation of nanoclusters, which could be employed for the discovery of new clusters. More interestingly, even though Au_{18} product was identified in both pH 5.25 and pH 8 solutions, pH effect on the transformation pathway was evidenced. After adjusting the pH to 8, the significant decrease of activation barrier from 30.0 ± 2.2 kcal/mol to 19.3 ± 1.5 kcal/mol and the change to the negative sign of entropy were obtained. This could be ascribed to the change in the ligand zwitterionic nature, which is proved by the increase in the number of sodium ions on the ligands in ESI spectra. The sensitivity of the cluster transformation to the surface was further studied by adding 5.5eq free GSH to the as isolated Au_{22} solution. Alternation of transformation pathway and product were suggested from the drastic drop in activation barrier to 12.7 ± 0.7 kcal/mol, as well as the Au_{15} and Au_{10-12} products identified in ESI spectra. Sensitivity of cluster transformation to the surface revealed herein enables the prediction on the fate of nanocluster in catalysis, energy, and biological applications.

ASSOCIATED CONTENT

Supporting Information

Additional ESI-MS, PAGE separation, UV-vis data along with other content as described in the text supplied as Supporting Information, Characterization data is available free of charge on the ACS Publications website.

AUTHOR INFORMATION

Corresponding Author

p_yang@berkeley.edu

Author Contributions

All authors have given approval to the final version of the manuscript.

ACKNOWLEDGMENT

ABBREVIATIONS

GSH, glutathione; PAGE, polyacrylamide gel electrophoresis.

REFERENCES

(1) Jin, R.; Zeng, C.; Zhou, M.; Chen, Y. Atomically Precise Colloidal Metal Nanoclusters and Nanoparticles: Fundamentals and Opportunities. *Chem. Rev.* **2016**, *116* (18), 10346–10413.

(2) Abbas, M. A.; Kim, T. Y.; Lee, S. U.; Kang, Y. S.; Bang, J. H. Exploring Interfacial Events in Gold-Nanocluster-Sensitized Solar Cells: Insights into the Effects of the Cluster Size and Electrolyte on Solar Cell Performance. *J. Am. Chem. Soc.* **2016**, *138* (1), 390–401.

(3) Du, B.; Jiang, X.; Das, A.; Zhou, Q.; Yu, M.; Jin, R.; Zheng, J. Glomerular Barrier Behaves as an Atomically Precise Bandpass Filter in a Sub-Nanometre Regime. *Nat. Nanotechnol.* **2017**, *12* (11), 1096–1102.

(4) García, C.; Pollitt, S.; van der Linden, M.; Truttmann, V.; Rameshan, C.; Rameshan, R.; Pittenauer, E.; Allmaier, G.; Kregsamer, P.; Stöger-Pollach, M.; Barrabes, N.; Rupprechter, G. Support Effect on the Reactivity and Stability of $Au_{25}(SR)_{18}$ and $Au_{144}(SR)_{60}$ Nanoclusters in Liquid Phase Cyclohexane Oxidation. *Catal. Today* **2019**, *336* (01 October), 174-185.

(5) Zhang, J.; Li, Z.; Huang, J.; Liu, C.; Hong, F.; Zheng, K.; Li, G. Size Dependence of Gold Clusters with Precise Numbers of Atoms in Aerobic Oxidation of D-Glucose. *Nanoscale* **2017**, *9* (43), 16879–16886.

(6) Li, G.; Jiang, D. E.; Kumar, S.; Chen, Y.; Jin, R. Size Dependence of Atomically Precise Gold Nanoclusters in Chemoselective Hydrogenation and Active Site Structure. *ACS Catal.* **2014**, *4* (8), 2463–2469.

(7) Dreier, T. A.; Wong, O. A.; Ackerson, C. J. Oxidative Decomposition of $Au_{25}(SR)_{18}$ Clusters in a Catalytic Context. *Chem. Commun.* **2015**, *51* (7), 1240–1243.

(8) Knoppe, S.; Dolamic, I.; Burgi, T. Racemization of a Chiral Nanoparticle Evidences the Flexibility of the Gold-Thiolate Interface. *J. Am. Chem. Soc.* **2012**, *134* (31), 13114–13120.

(9) Varnholt, B.; Dolamic, I.; Knoppe, S.; Bürgi, T. On the Flexibility of the Gold-Thiolate Interface: Racemization of the $Au_{40}(SR)_{24}$ Cluster. *Nanoscale* **2013**, *5* (20), 9568–9571.

(10) Zeng, C.; Chen, Y.; Das, A.; Jin, R. Transformation Chemistry of Gold Nanoclusters: From One Stable Size to Another. *J. Phys. Chem. Lett.* **2015**, *6* (15), 2976–2986.

(11) Zeng, C. J.; Liu, C. Y.; Pei, Y.; Jin, R. C. Thiol Ligand-Induced Transformation of $Au_{38}(SC_2H_4Ph)_{24}$ to $Au_{36}(SPh-t-Bu)_{24}$. *ACS Nano* **2013**, *7* (7), 6138–6145.

(12) Dainese, T.; Antonello, S.; Bogialli, S.; Fei, W.; Venzo, A.; Maran, F. Gold Fusion: From $Au_{25}(SR)_{18}$ to $Au_{38}(SR)_{24}$, the Most Unexpected Transformation of a Very Stable Nanocluster. *ACS Nano* **2018**, *12* (7), 7057–7066.

(13) Higaki, T.; Liu, C.; Chen, Y.; Zhao, S.; Zeng, C.; Jin, R.; Wang, S.; Rosi, N. L.; Jin, R. Oxidation-Induced Transformation of Eight-Electron Gold Nanoclusters: $[Au_{23}(SR)_{16}]^-$ to $[Au_{28}(SR)_{20}]^0$. *J. Phys. Chem. Lett.* **2017**, *8* (4), 866–870.

(14) Song, Y.; Abroshan, H.; Chai, J.; Kang, X.; Kim, H. J.; Zhu, M.; Jin, R. Molecular-like Transformation from PhSe-Protected Au_{25} to Au_{23} Nanocluster and Its Application. *Chem. Mater.* **2017**, *29* (7), 3055–3061.

(15) Luo, Z.; Nachammai, V.; Zhang, B.; Yan, N.; Leong, D. T.; Jiang, D. E.; Xie, J. Toward Understanding the Growth Mechanism: Tracing All Stable Intermediate Species from Reduction of Au(I)-Thiolate Complexes to Evolution of Au_{25} Nanoclusters. *J. Am. Chem. Soc.* **2014**, *136* (30), 10577–10580.

(16) Yao, Q.; Yuan, X.; Fung, V.; Yu, Y.; Leong, D. T.; Jiang, D. E.; Xie, J. Understanding Seed-Mediated Growth of Gold Nanoclusters at Molecular Level. *Nat. Commun.* **2017**, *8* (1), 1–10.

(17) Itteboina, R.; Madhuri, U. Di.; Ghosal, P.; Kannan, M.; Sau, T. K.; Tsukuda, T.; Bhardwaj, S. Efficient One-Pot Synthesis and PH-Dependent Tuning of Photoluminescence and Stability of $Au_{18}(SC_2H_4CO_2H)_{14}$ Cluster. *J. Phys. Chem. A* **2018**, *122* (5), 1228–1234.

(18) Malola, S.; Häkkinen, H. Chiral Inversion of Thiolate-Protected Gold Nanoclusters via Core Reconstruction without Breaking a Au-S Bond. *J. Am. Chem. Soc.* **2019**, *141* (14), 6006–6012.

(19) Yu, Y.; Luo, Z. T.; Chevrier, D. M.; Leong, D. T.; Zhang, P.; Jiang, D. E.; Xie, J. P. Identification of a Highly Luminescent $Au_{22}(SG)_{18}$ Nanocluster. *J. Am. Chem. Soc.* **2014**, *136* (49), 17355.

(20) Zhang, H.; Liu, H.; Tian, Z.; Lu, D.; Yu, Y.; Cestellos-Blanco, S.; Sakimoto, K. K.; Yang, P. Bacteria Photosensitized by Intracellular Gold Nanoclusters for Solar Fuel Production. *Nat. Nanotechnol.* **2018**, *13* (10), 900–905.

(21) Zhang, C.; Zhang, A.; Hou, W.; Li, T.; Wang, K.; Zhang, Q.; De La Fuente, J. M.; Jin, W.; Cui, D. Mimicking Pathogenic Invasion with the Complexes of $Au_{22}(SG)_{18}$-Engineered Assemblies and Folic Acid. *ACS Nano* **2018**, *12* (5), 4408–4418.

(22) Pyo, K.; Ly, N. H.; Yoon, S. Y.; Shen, Y.; Choi, S. Y.; Lee, S. Y.; Joo, S. W.; Lee, D. Highly Luminescent Folate-Functionalized Au_{22} Nanoclusters for Bioimaging. *Adv. Healthc. Mater.* **2017**, *6* (16), 1–8.

(23) Negishi, Y.; Nobusada, K.; Tsukuda, T. Glutathione-Protected Gold Clusters Revisited: Bridging the Gap between Gold(I)-Thiolate Complexes and Thiolate-Protected Gold Nanocrystals. *J. Am. Chem. Soc.* **2005**, *127* (14), 5261–5270..

(24) Moaseri, E.; Bollinger, J. A.; Changalvaie, B.; Johnson, L.; Schroer, J.; Johnston, K. P.; Truskett, T. M. Reversible Self-Assembly of Glutathione-Coated Gold Nanoparticle Clusters via PH-Tunable Interactions. *Langmuir* **2017**, *33* (43), 12244–12253.

(25) Yu, Y.; Li, J.; Chen, T.; Tan, Y. N.; Xie, J. Decoupling the CO-Reduction Protocol to Generate Luminescent $Au_{22}(SR)_{18}$ Nanocluster. *J. Phys. Chem. C* **2015**, *119* (20), 10910–10918.

(26) Yu, Y.; Chen, X.; Yao, Q.; Yu, Y.; Yan, N.; Xie, J. Scalable and Precise Synthesis of Thiolated Au_{10-12}, Au_{15}, Au_{18}, and Au_{25} Nanoclusters via PH Controlled CO Reduction. *Chem. Mater.* **2013**, *25* (6), 946–952.

(27) Taylor, M. G.; Mpourmpakis, G. Thermodynamic Stability of Ligand-Protected Metal Nanoclusters. *Nat. Commun.* **2017**, *8* (May), 1–8.

(28) Love, J. C.; Estroff, L. A.; Kriebel, J. K.; Nuzzo, R. G.; Whitesides, G. M. Self-Assembled Monolayers of Thiolates on Metals as a Form of Nanotechnology. *Chem. Rev.* **2005**, *105* (4), 1103–1169.

(29) Chan, B.; Yim, W. L. Accurate Computation of Cohesive Energies for Small to Medium-Sized Gold Clusters. *J. Chem. Theory Comput.* **2013**, *9* (4), 1964–1970.

(30) Knoppe, S.; Michalet, S.; Bürgi, T. Stabilization of Thiolate-Protected Gold Clusters against Thermal Inversion: Diastereomeric $Au_{38}(SCH_2CH_2Ph)_{24-2x}$(R - BINAS)$_x$. *J. Phys. Chem. C* **2013**, *117* (29), 15354–15361.